FACTA UNIVERSITATIS
Series: **Electronics and Energetics** Vol. 37, Nº 2, June 2024, pp. 369 - 389
https://doi.org/10.2298/FUEE2402369K

Original scientific paper

PERFORMANCE ANALYSIS OF PLL CONTROL STRATEGIES ON GRID CONNECTED PV SYSTEM UNDER DISTURBED GRID CONDITIONS

Aakriti Khanna[1], Anjali Garg[1], Shradha Singh Parihar[2]

[1]The NorthCap University, Gurugram, India
[2]Greater Noida Institute of Technology, Greater Noida, India

ORCID iDs:	Aakriti Khanna	https://orcid.org/0000-0003-2792-3473
	Anjali Garg	https://orcid.org/0000-0001-8157-0379
	Shradha Singh Parihar	https://orcid.org/0000-0001-8809-4504

Abstract. *The rising demand for renewable energy, particularly solar power, stems from its immediate availability and the imperative to curb carbon emissions associated with fossil fuel consumption. Consequently, there has been a significant surge in the installation and development of grid-connected Photovoltaic (PV) systems. However, integrating PV sources with the grid presents various challenges related to power quality. This article aims to explore how grid-connected PV systems perform when faced with different disruptions within the grid. To address this, a novel Dual Sliding Fourier Transform (DSFT) Phase-Locked Loop (PLL) control strategy has been proposed. The methodology involves modeling a typical grid-connected PV system. The proposed and conventional control strategies to regulate the grid-connected inverter have been implemented under four distinct disturbed conditions: frequency disturbance, harmonic disturbance, phase jump disturbance, and DC offset disturbance. This approach is further compared with the traditional techniques, namely Dual Second Order Generalized Integrator (DSOGI PLL) and decoupled stationary reference frame (dαβ PLL). The evaluation criterion considers the time required to track frequency changes, mitigation of harmonics, and accuracy in phase error estimation. The findings reveal that the DSFT PLL control strategy outperforms the conventional techniques across all four disturbed conditions in the context of grid-connected PV systems.*

Key words: *Disturbed condition, Grid connected PV system, control strategies, PLL, Inverter*

Received November 20, 2023; revised January 09, 2024; accepted January 14, 2024
Corresponding author: Aakriti Khanna
The NorthCap University, Gurugram, India
E-mail: aaki.0502@gmail.com

1. INTRODUCTION

1.1. Motivation

In recent times, fossil fuels have been the main source of power generation. Due to extreme change in the environmental conditions and the incessant demand for energy, renewable energy sources are gaining unprecedented interest. Renewable energy sources play a pivotal role in the realm of energy generation, standing prominently as a key contributor to the global energy landscape. These sources, which harness naturally replenishing elements such as sunlight, wind, water, and geothermal heat, have become increasingly integral to addressing the growing demand for sustainable and environmentally friendly energy solutions [1, 2]. Solar energy, being an inexhaustible source of energy, is a good renewable energy source. Here, the solar energy by the use of PV cells converts the solar or the PV energy into electrical energy. The connection of PV with grid represents a pivotal advancement in renewable energy integration. However, the grid integration comes with various issues posing a number of problems related to power quality, equipment disruption, complete failure of the grid connected system. Hence, it is obligatory to overcome the disturbances for the safe working of grid connected systems.

1.2. Literature Survey

The organization of PV cells into modules that are interconnected into various configurations for optimizing the tracking of maximum power for the generation of electrical energy has been discussed in [3-6]. For the effective utilization of PV power, PV systems are integrated with grid. Authors in [7-11] discussed about the need of PV arrays and inverters for the grid connection. Various consequences of power electronic converters have been presented in [12].

The increased usage of nonlinear loads which include compact fluorescent lamps (CFLs), power electronics interfaced converters, etc. deteriorates the power quality and increases the harmonic distortion of the grid connected PV system [13]. The synchronous reference frame phase-locked loop (SRF PLL) [14] is a commonly employed method for achieving grid synchronization in a grid-connected voltage source inverter (VSI). Its purpose is to precisely determine the parameters of voltage, frequency, and phase angle under conditions of balanced grid voltage as demonstrated in [15]. But, unfortunately, under unbalanced conditions, the results of SRF-PLL produce errors; hence, they will not be able to accurately track the parameters thereby affecting the stability of the grid connected PV system. To overcome the drawback of conventional SRF-PLL, many researchers have examined several types of modified SRF-PLL including double decoupled SRF-PLL (DDSRF-PLL) [16], second order generalized integrator PLL (SOGI-PLL) [17], double second order generalized integrator (DSOGI-PLL) which works well for strong grids, but may harm equipment with weak grids [18], mixed second and third order generalized integrator PLL (MSTOGI-PLL) [19]. The DDSRF-PLL extracts positive and negative components from grid voltages, thereby obtaining better results of PLL by using a decoupling network. However, the control algorithm of DDSRF-PLL is complex to implement. SOGI PLL is sensitive to variations (Sensitive to DC Offset and low order harmonics), thus leading to a very poor dynamic response. The MSTOGI-PLL method presented in [19], eliminates the dc offset of input signals in the SOGI. However, it affects filtering capability, requires high bandwidth for fast response and has poor dynamic performance. Sliding mode based control for the LCL grid inverters has been analyzed in [20]

providing satisfactory performance but with a drawback of higher overshoots in responses. Dαβ PLL works well in the presence of unbalanced grid voltages [21]. Various asynchronous techniques are also being researched and are compared with PLL based techniques in [22].

1.3. Paper Contributions

It has been seen from the existing literature survey, that most researchers consider only PID tuning to give a trade-off condition having a single disturbance in the grid for the analysis of the control technique. In this article, four different types of disturbances are considered for the evaluation of the presented novel control strategy. The major contributions of this research paper are mentioned below:

1) A new control strategy Dual Sliding Fourier Transform (DSFT) has been developed for the first time which takes Fourier transformation into consideration playing a crucial role in frequency tracking. Here, the Fourier transform identifies the grid frequency without compromising the power system's overall stability and reliability.
2) The proposed control strategy has been tested for four disturbances: frequency disturbance, harmonic disturbance, phase jump disturbance and DC offset disturbance.
3) Simulink model of the proposed strategy (DSFT) has been implemented and compared with traditional control techniques (DSOGI PLL and dαβ PLL) to validate the effectiveness and are found to be beneficial for grids polluted with different types of disturbances.
4) The results attained in the research paper result in high immunity of the grid connected structure and elimination of complex PID controller tuning.

1.4. Paper Organization

The article is organized as follows: In Section 2, description of the grid connected PV system is presented, Section 3 comprises the control strategies, the result analysis has been done in Section 4 and Section 5 summarizes the paper along with the future scope of the proposed control technique.

2. DESCRIPTION OF PV SYSTEM

The block diagram depicting grid connected Photovoltaic system is shown in Fig. 1 which comprises of PV array, DC-DC Boost converter, DC-AC converter (inverter), control strategy for the pulses of the inverter, loads and grid.

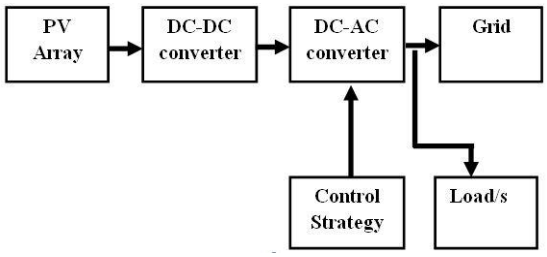

Fig. 1 Block Diagram of grid connected PV system

PV array converts daylight (irradiance) into electricity. The PV Array, shown in Fig.1, generates 33.4 KW of maximum power having 9 parallel strings; each string has 17 modules connected in series. The number of cells per module are 60 having an open circuit voltage (V_{oc}) of 36.6V, short circuit current (I_{sc}) of 7.97A, maximum power point voltage (V_{mpp}) of 29.3V and maximum power point current (I_{mpp}) of 7.47A. DC-DC converter used is the boost converter, required to boost the PV voltage to tone with DC link voltage. DC-AC converter used in the grid connection takes the DC input and converts it into AC. It molds the current into sinusoidal waveform in a way that it can be fed into the electric utility grid.

Fig. 2 presents the structure of a 3-phase inverter used in Grid connected PV system. Here, the inverter performs the function of frequency synchronization and maintenance of DC-link voltage. The topology uses six insulated gate bi-polar transistor (IGBT) switches connected in bridge configuration (these switches are considered to be ideal, i.e., balanced voltages and constant dc link voltage). Inverters also add layer for the protection of devices from power outages, over-voltage and over current.

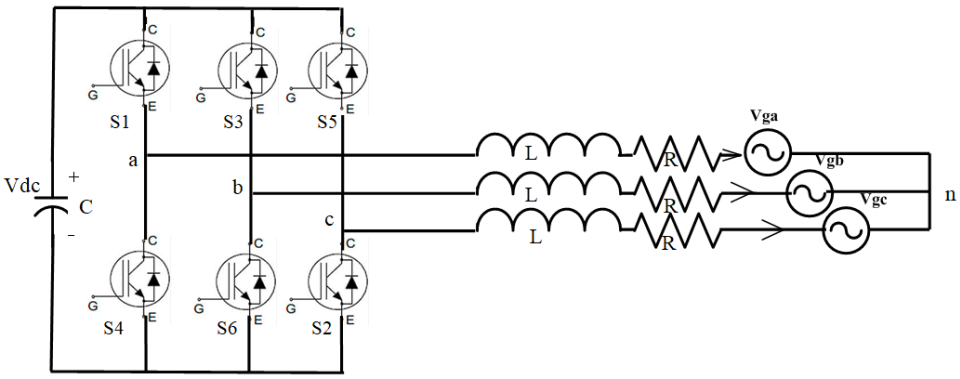

Fig. 2 Three phase grid connected inverter [23]

The grid under examination in this paper is regarded as a contaminated unit that has been intentionally subjected to various disturbances. All the disturbances like frequency variation, harmonic distortion, phase jump and DC offset disturbance have been introduced to analyze their impact on the grid's performance.

3. CONTROL STRATEGIES

This paper deals with different control strategies, namely:

3.1. Traditional Control Strategies:

3.1.1. DSOGI PLL

3.1.2. dαβ PLL

3.2. Proposed Dual Sliding Fourier Transform (DSFT) PLL and its implementation

3.1. Traditional Control Strategies

Traditional control strategies considered in this paper are DSOGI PLL and dαβ PLL for the reason that these have been widely used in the literature by the researchers.

3.1.1. DSOGI PLL

Dual Second Order Generalized Integrator (DSOGI-PLL) [24] control strategy translates the three-phase voltage from the abc to αβ reference frame. A positive sequence calculator is used to extract the positive sequence voltage components of αβ frame as shown in Fig. 3.These are then translated to dq reference frame. Here, SRF PLL is employed to achieve phase locking by closed-loop control of the q-axis component of voltage. However, DSOGI PLL is not suitable for weak grids, has large convergence time, has high frequency overshoot and may harm grid connected equipments.

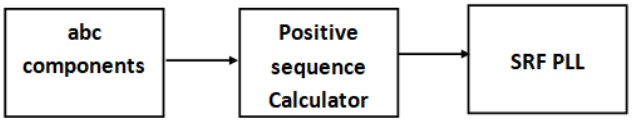

Fig. 3 Structure of DSOGI PLL

3.1.2. dαβ PLL

dαβ PLL [25] refers to decoupled stationary reference frame PLL which has evolved from the combination of decoupled double synchronous reference frame PLL (DDSRF PLL) and stationary reference frame PLL (αβ PLL) strategies. dαβ PLL uses decoupling of voltage sequence from DDSRF PLL and uses αβ PLL algorithm for estimation of phase angle. The structure of dαβ PLL is shown in Fig. 4 [25]. The benefit of dαβ PLL is that it works with distortions, which is the drawback of SRF PLL. However, it suffers from high overshoot of phase angle tracking error when a fault occurs and has non immunity to DC offset and harmonics.

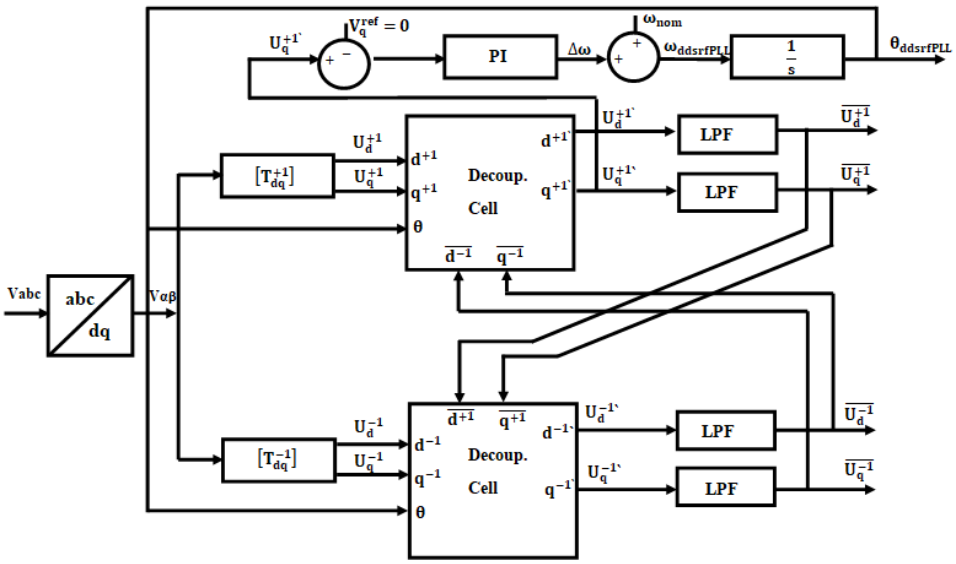

Fig. 4 Structure of dαβ PLL [25]

3.2. Proposed Dual Sliding Fourier Transform PLL and its implementation

In this paper, Dual Sliding Fourier Transform (DSFT) PLL control strategy has been proposed. DSFT PLL aims to overcome the drawbacks of Sliding Fourier Transform (SFT) technique [26], [27] involving long settling time, requirement of PID tuning, elimination of harmonics, etc. Here, two stages of SFT are connected in such a way that fast and accurate estimate of frequency variation is detected. For example, if there is a sudden change in the frequency of the grid, the controller is designed in such a way that the model tracks the change within the shortest time. The estimated frequency of the first stage of DSFT PLL defines the window size for the second stage of DSFT PLL. Mathematical analysis of SFT PLL which forms the base for DSFT PLL is presented using (1) to (25).

A balanced set of three phase sinusoidal voltage Vg is considered as grid voltages for the three phases with E (volts), being the peak value and f_g (Hz) being the frequency. V_g is given in (1).

$$\begin{aligned} V_{ga} &= E\sin(2\pi f_g t + \theta) \\ V_{gb} &= E\sin(2\pi f_g t - \tfrac{2\pi}{3} + \theta) \\ V_{gc} &= E\sin(2\pi f_g t + \tfrac{2\pi}{3} + \theta) \end{aligned} \tag{1}$$

where, θ represents the initial phase shift (radians) of voltage V_{ga}, f_g is assumed constant for the analysis.

The three-phase voltages undergo processing through sine and cosine filters employing the principle of orthogonal signal generation as outlined in [28-30]. The filtering is done based on the assumption that the filters are made using two orthogonal sets of balanced equations, which originally have same grid phase sequence, running at nominal (pre-known) frequency f_n (Hz), having unity amplitude.

The first set is called as direct set or the sine set, represented by V_{cx}, given by sine functions as shown in (2).

$$\begin{aligned} V_{cax} &= \sin(2\pi f_n t) \\ V_{cbx} &= \sin(2\pi f_n t - \tfrac{2\pi}{3}) \\ V_{ccx} &= \sin(2\pi f_n t + \tfrac{2\pi}{3}) \end{aligned} \tag{2}$$

The second set is called as quadratic set or the cosine set, represented by V_{cy}, given by cosine functions as shown in (3).

$$\begin{aligned} V_{cay} &= \cos(2\pi f_n t) \\ V_{cby} &= \cos(2\pi f_n t - \tfrac{2\pi}{3}) \\ V_{ccy} &= \cos(2\pi f_n t + \tfrac{2\pi}{3}) \end{aligned} \tag{3}$$

Fourier transform is applied on the (1) - (3) using the integrations given by (4) and (5), which are the compact versions for the three phases, here, i = a,b,c (three phases) and T_n is the time period, given by $T_n = 1/f_n$.

$$x_i = \frac{1}{T_n}\int_t^{t+T_n} v_{cix}\, v_{gi}\, dt \tag{4}$$

$$y_i = \frac{1}{T_n}\int_t^{t+T_n} v_{ciy}\, v_{gi}\, dt \tag{5}$$

For f_n being any positive and a non-zero value, two cases will arise while solving the integrals:

Case (i): when the value of two frequencies are not equal i.e. $f_g \neq f_n$(off-nominal frequency case)

Case (ii): arises when $f_g = f_n$ (nominal frequency case).

Case (i): The case of 'off-nominal frequency'

For $|f_g\text{-}f_n| < f_n$, x_i and y_i, the active component (direct) and reactive component (quadratic) are functions of frequencies and time as follows:

For Phase A:

$$x_a(t) = k_1 \cos[w_D t + \theta + \Delta\theta_1] - k_2 \cos[w_T t + \theta + \Delta\theta_2] \quad (6)$$

$$y_a(t) = k_1 \sin[w_D t + \theta + \Delta\theta_1] + k_2 \sin[w_T t + \theta + \Delta\theta_2] \quad (7)$$

For Phase B:

$$x_b(t) = k_1 \cos[w_D t + \theta + \Delta\theta_1] - k_2 \cos[w_T t + \theta + \Delta\theta_2 + \tfrac{2\pi}{3}] \quad (8)$$

$$y_b(t) = k_1 \sin[w_D t + \theta + \Delta\theta_1] + k_2 \sin[w_T t + \theta + \Delta\theta_2 + \tfrac{2\pi}{3}] \quad (9)$$

For Phase C:

$$x_c(t) = k_1 \cos[w_D t + \theta + \Delta\theta_1] - k_2 \cos[w_T t + \theta + \Delta\theta_2 - \tfrac{2\pi}{3}] \quad (10)$$

$$y_c(t) = k_1 \sin[w_D t + \theta + \Delta\theta_1] + k_2 \sin[w_T t + \theta + \Delta\theta_2 - \tfrac{2\pi}{3}] \quad (11)$$

where,

$$w_D = 2\pi(f_g - f_n) \quad (12)$$

$$w_T = 2\pi(f_g + f_n) \quad (13)$$

$$\Delta\theta_1 = \frac{w_D}{2f_n} \quad (14)$$

$$k_1 = \frac{E\sin(\Delta\theta_1)}{2\Delta\theta_1} \quad (15)$$

$$\Delta\theta_2 = \frac{w_T}{2f_n} \quad (16)$$

$$k_2 = \frac{E\sin(\Delta\theta_2)}{2\Delta\theta_2} \quad (17)$$

Equations (6) to (11) represent the active and reactive components for the three phases comprising of two sinusoidal terms. It is observed from these set of equations that one of the sine term has higher magnitude (k_1) and lower frequency (w_D), while the second sine term has lower magnitude (k_2) and higher frequency (w_T). From (6), (8) and (10), it is evident that these are for balanced set of three phases in cosine terms which results in zero sum. Similarly, the second terms of (7), (9) and (11) show that these are for balanced set of three phases in sine terms which results in zero sum.

Hence, the sum of the two components x_i and y_i(active and reactive) are calculated and given by (18) and (19), respectively.

$$x_i = \sum_{i=a}^{c} 3k_1 \cos[w_D t + \theta + \Delta\theta_1] \quad (18)$$

$$y_i = \sum_{i=a}^{c} 3k_1 \sin[w_D t + \theta + \Delta\theta_1] \quad (19)$$

Equation (20) is obtained by dividing (19) by (18).

$$\frac{y_i}{x_i} = \tan[w_D t + \theta + \Delta\theta_1] \tag{20}$$

Substituting (12) in (20), we get (21).

$$2\pi(f_g - f_n)t + \theta + \Delta\theta_1 = \tan^{-1}\frac{y_t}{x_t} \tag{21}$$

Rearranging (21) and using (1), the phase angle for the first phase θ_a can be obtained and given by (22).

$$\theta_a = 2\pi f_g t + \theta = \tan^{-1}\frac{y_t}{x_t} + 2\pi f_n t - \Delta\theta_1 \tag{22}$$

Equation (23) can be obtained by substituting (14) and (12) in (22).

$$\theta_a = \tan^{-1}\frac{y_t}{x_t} + 2\pi f_n t - \frac{\pi(f_g - f_n)}{f_n} \tag{23}$$

As f_g is a constant value, so

$$\frac{\Delta f_g}{\Delta t} = 0$$

where $\Delta\theta_1$ and θ both are constants, so, their time derivatives will be zero. Therefore, the value of f_g can be calculated by taking the time derivative of (22) and is given in (24):

$$f_g = \frac{1}{2\pi}\frac{d}{dt}\left(\tan^{-1}\frac{y_t}{x_t}\right) + f_n \tag{24}$$

As f_g is estimated, θ can be estimated using (22) and $\Delta\theta_1$ can be estimated using (14). E, the peak value of the voltage, can then be estimated with the help of (15), (18) and (19) and is given in (25):

$$E = \frac{2}{3}\frac{\Delta\theta_1}{\sin(\Delta\theta_1)}\sqrt{{x_t}^2 + {y_t}^2} \tag{25}$$

where, $\frac{\Delta\theta_1}{\sin(\Delta\theta_1)}$ is the magnitude correction factor and $\frac{2}{3}\sqrt{{x_t}^2 + {y_t}^2}$ is the uncompensated magnitude.

Case (ii): The case of 'Nominal frequency'

For $f_g = f_n$, using (23), the phase angle θ_a of grid voltage V_{ga} is expressed as (26)

$$\theta_a = 2\pi f_g t + \theta = \tan^{-1}\frac{y_t}{x_t} + 2\pi f_n t \tag{26}$$

This makes case (ii) as a special case of the off-nominal case (i).

3.2.1. Implementation of the Proposed Dual Sliding Fourier Transform PLL

In DSFT PLL, the second stage Fourier transform finds its filter frequency using the grid frequency determined from the first stage.

Fig. 5 presents the generation of x_i and y_i using (4) and (5) wherein the value gets updated with every sample of grid voltage. To update the integrals, constant width delays are considered. The formulation of active and reactive components for the three phases using SFT is shown in Fig. 6.

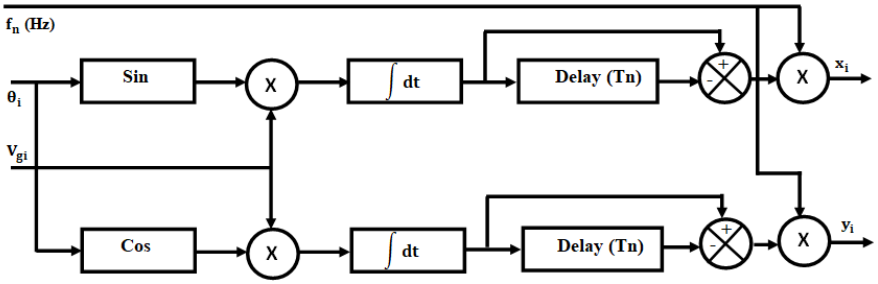

Fig. 5 Schematic representation of integrals for SFT

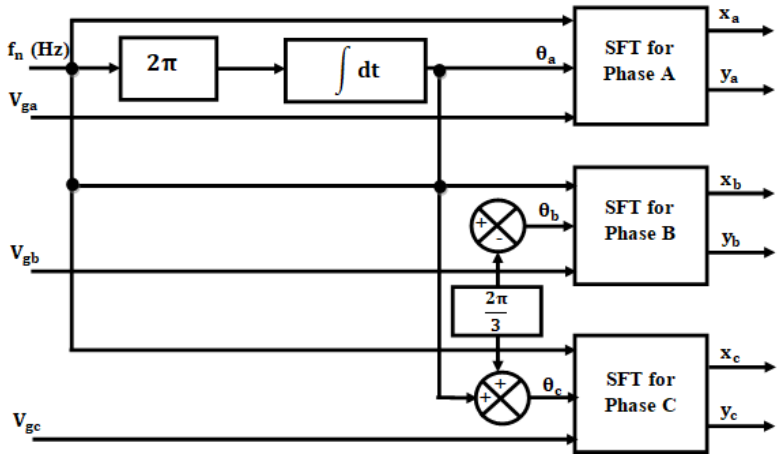

Fig. 6 Active and reactive components of three phase voltage using SFT

Grid frequency is estimated using (24) in the stage 1 i.e. using the first SFT. The schematic representation of grid frequency is depicted in Fig. 7.

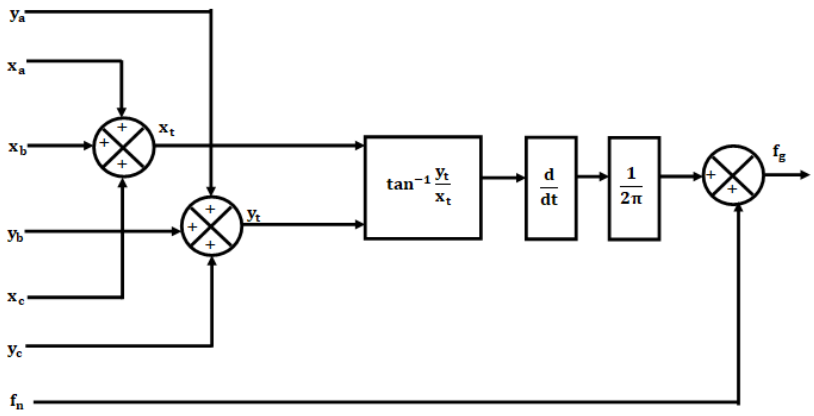

Fig. 7 Estimation of grid frequency using SFT

Fig. 8 presents the proposed system of DSFT PLL. In this, stage 1 SFT has fixed window width i.e. the delay is fixed. This provides the estimate of actual frequency (f_{gi} in Fig. 8) of grid voltage. This estimated frequency is then filtered using Filter 1 in order to attenuate the ripples of high frequency. The output of this filter (f_{gif} in Fig. 8) is then passed to the stage 2 SFT where the size of the window is variable. The filter output of Filter 1 controls the duration of the delay needed. The filtered frequency is integrated in order to find the filter phase angle. This drives the sine/cosine filters of second stage SFT. The output frequency, f_{gii} from stage 2 is also filtered using Filter 2 to get a smooth estimate of grid frequency. The output phase angle from second stage is added to the filter phase angle in order to estimate the required grid positive sequence phase angle.

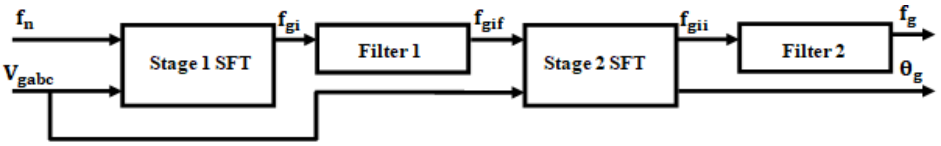

Fig. 8 Structure of proposed DSFT PLL

4. RESULTS

The proposed control strategy has been simulated for grid connected PV system and is compared with dαβ PLL and DSOGI PLL in MATLAB Simulink. The simulink model of the proposed strategy implemented in MATLAB/Simulink is presented in Fig. 9. Fig. 9(a) shows the overall structure of proposed control strategy, whereas, Fig. 9 (b) depicts the detailed internal structure of DSFT block where the two stages of SFT and two filters have been used for the estimation of phase and frequency. The simulation parameters for the proposed strategy are tabulated in Table 1**.** Here, the simulations are carried out for four disturbed conditions: frequency disturbance, harmonic disturbance, phase jump disturbance and DC offset disturbance.

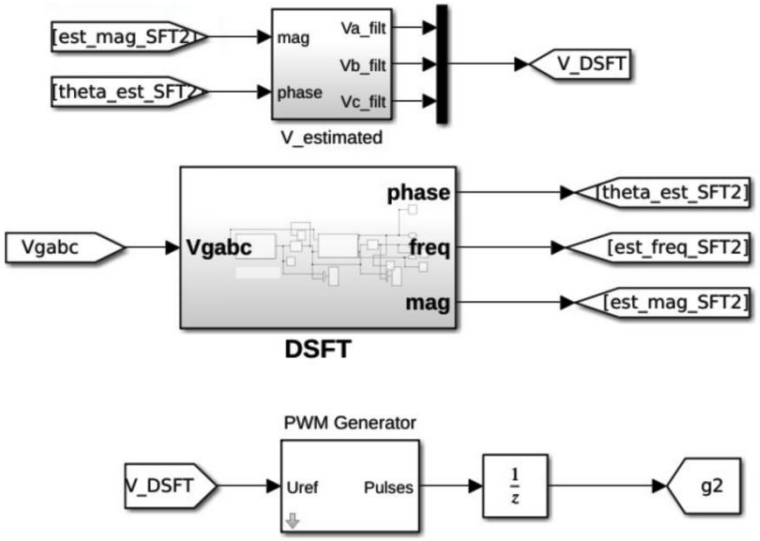

Fig. 9(a) Simulink model of proposed control strategy

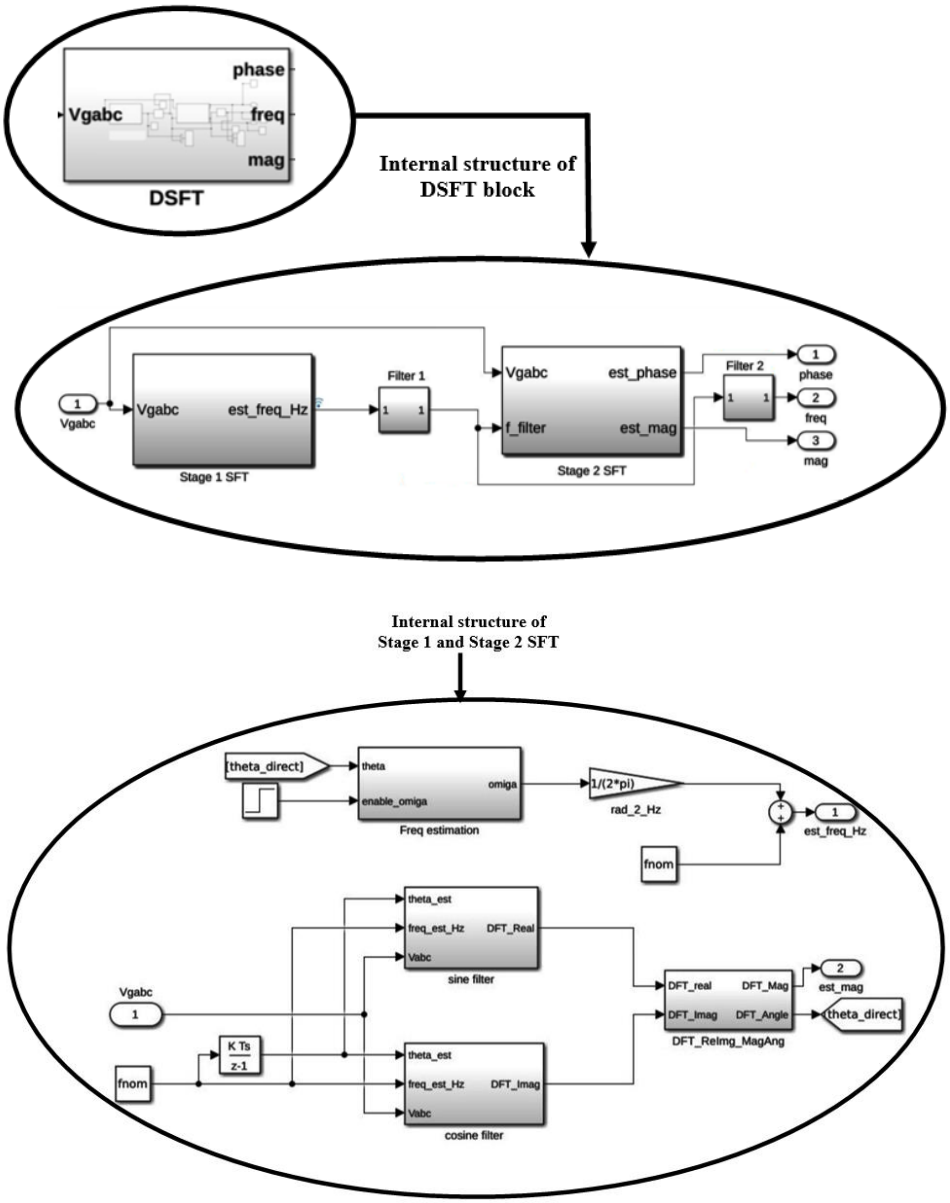

Fig. 9(b) Internal Structure of DSFT block

Fig. 9 Implementation of proposed control strategy

Table 1 Simulation parameters for proposed strategy

Parameter	Value
Frequency, fnom (Hz)	50
Sample time, Ts (sec)	0.00015625
pi	3.14
Step time (s)	2/fnom
Gain, K	0.7071

where fnom is the nominal frequency (the frequency on which the control strategy has been built), Ts is the sample time of the control strategy, step time is the time given to the step generator for enabling the input and K is the gain involved in the estimation of theta.

4.1. Frequency Disturbance

Frequency disturbance deals with shift in grid frequency from 50 Hz to a different value. Here, the frequency is disturbed for two conditions (a) long duration frequency distortion with a shift in frequency from 50 Hz to 50.34 Hz and (b) short duration frequency distortion with a shift in grid frequency from 50 Hz to 52 Hz. Fig. 10 and Fig. 11 shows the frequency comparison and phase error comparison respectively with frequency distortion as a grid disturbance.

4.1.1. Long duration frequency disturbance from 0.2 sec to 1.0 sec

Here, frequency disturbance is given for a long duration of 0.8 seconds and has been analyzed for three different control strategies (proposed DUAL SFT (DSFT) PLL, DSOGI PLL and dαβ PLL). Fig. 10 and Fig. 11 illustrate the comparison of PLL techniques considering frequency disturbance in terms of frequency and phase error respectively. Fig. 10 infers that DSFT PLL control strategy took 0.02 seconds to track the frequency change; DSOGI PLL strategy took 0.1 seconds to track whereas dαβ PLL strategy took around 0.3 seconds to track the frequency change. From Fig.11, we see that DSFT PLL settles the phase error in 0.02 seconds; DSOGI PLL settles the phase error in 0.15 seconds while dαβ PLL is unable to settle the phase error.

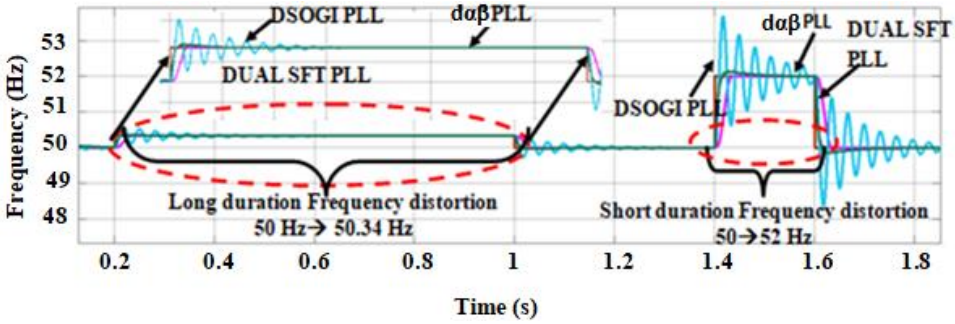

Fig. 10 Frequency comparison of PLL techniques with frequency disturbance

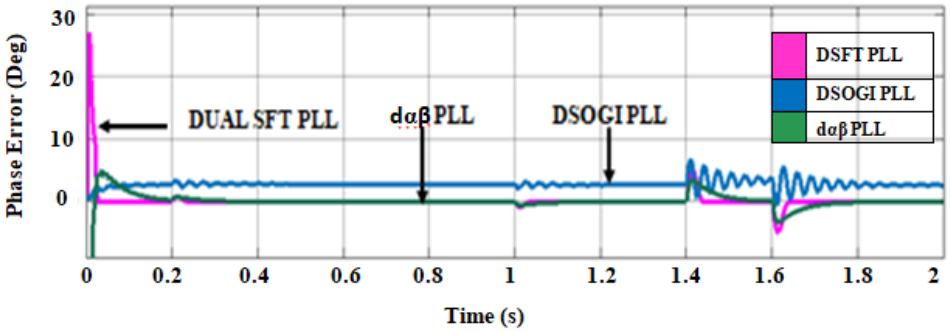

Fig. 11 Phase error comparison of PLL techniques with frequency disturbance

4.1.2. Short duration frequency disturbance from 1.4 sec to 1.6 sec

Here, the frequency disturbance prevails for a short duration of 0.2 seconds. Fig. 10 and Fig. 11 demonstrate the frequency and phase error comparison respectively for the three control strategies (proposed DSFT PLL, DSOGI PLL and dαβ PLL). It has been observed that DSFT PLL took the least time to track the change in frequency which is around 0.02 seconds, DSOGI PLL tracks the frequency change in around 0.1 seconds while dαβ PLL was unable to track from Fig. 10. In terms of the phase error comparison, Fig. 11 shows that DSFT PLL settles to zero in 0.02 seconds while DSOGI PLL took 0.15 seconds to settle and dαβ PLL was unable to settle. Comparative results obtained for the frequency disturbance in terms of frequency tracking time and phase error settling time are tabulated in Table 2.

Table 2 Comparison of control strategies for frequency disturbance

Type of Disturbance	Control Strategy	Frequency tracking time (sec)	Phase Error Settling time (Sec)
Long duration frequency disturbance (0.8 seconds)	Proposed DSFT PLL	0.02	0.02
	DSOGI PLL	0.1	0.15
	dαβ PLL	0.3	Unable to settle
Short duration frequency disturbance (0.2 seconds)	Proposed DSFT PLL	0.02	0.02
	DSOGI PLL	0.1	0.15
	dαβ PLL	Unable to track	Unable to track

4.2. Harmonic Disturbance

Harmonic disturbance, here, refers to the harmonic injections in the grid voltage [31-33]. The disturbance is analyzed in two categories (a) Injection of 3^{rd} and 5^{th} harmonic component with fundamental component and (b) Injection of 3^{rd}, 5^{th}, 7^{th} and 9^{th} harmonic component with fundamental component.

Fig. 12 (a) shows the grid voltage of phase A when 3^{rd} and 5^{th} harmonic component gets injected and Fig. 12 (b) shows the grid voltage of phase A when 3^{rd}, 5^{th}, 7^{th} and 9^{th} harmonic component gets injected as disturbance from 0.5 sec to 0.85 sec.

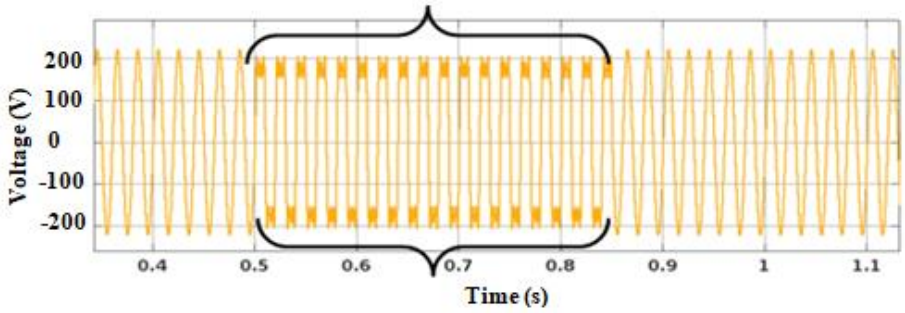

Fig. 12(a) Grid voltage with 3rd and 5th harmonic component injection in phase A

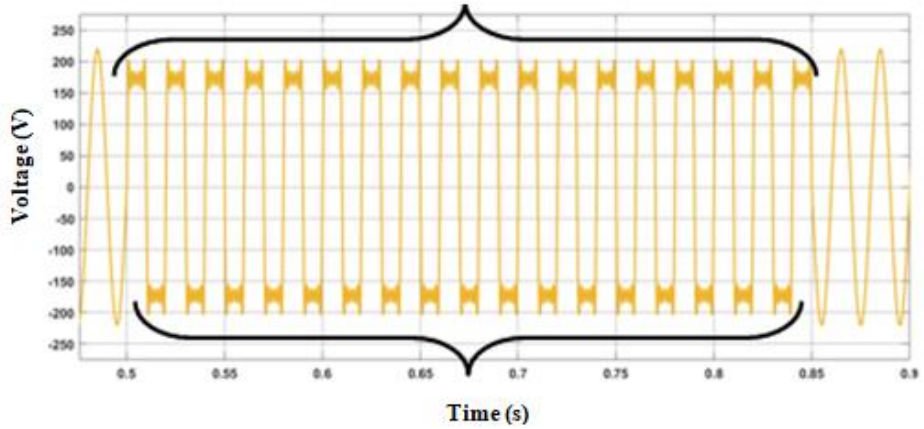

Fig. 12(b) Grid voltage with 3rd, 5th, 7th and 9th harmonic component injection in phase A

Fig. 12 Grid Voltage with harmonic components

The frequency comparison of the proposed DSFT PLL technique with the DSOGI PLL and dαβ PLL techniques for the disturbance period between 0.5 to 0.85 seconds is illustrated in Fig. 13. It clearly shows that for DSFT PLL, the frequency remains 50 Hz throughout the disturbance period while for the DSOGI PLL frequency varies in range of 49Hz-51Hz and for dαβ PLL, the range of variation of frequency is 44Hz-56Hz during the disturbance period.

The effect of PLL control techniques on the grid voltage during harmonic disturbance period is depicted in Fig. 14. Fig. 14(a), Fig. 14(b) and Fig. 14(c) display the grid voltage of the proposed control strategy DSFT PLL, DSOGI PLL strategy and dαβ PLL strategy respectively. It shows that DSFT PLL reconstructs the voltage, which was harmed during the injection of harmonics, DSOGI PLL reduces the amplitude of the grid voltage and dαβ is inefficient in removing the harmonics from the system. The output of dαβ PLL is non-sinusoidal in nature.

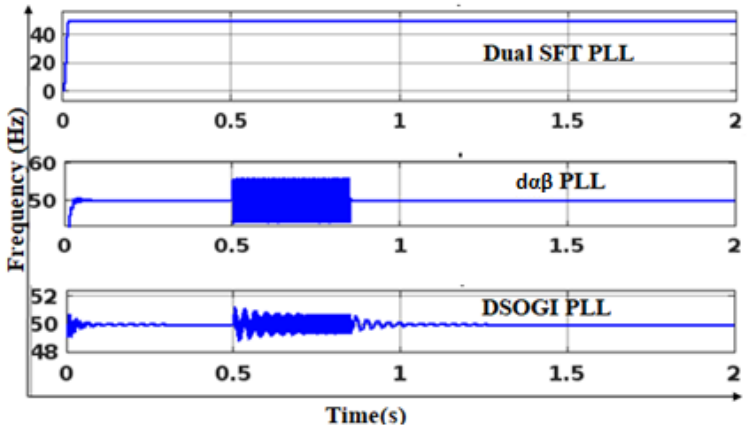

Fig. 13 Frequency comparison of PLL techniques with harmonic disturbance

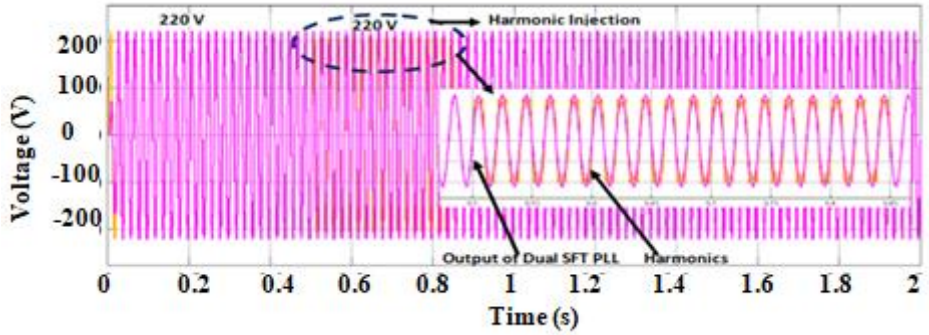

Fig. 14(a) Grid voltage with harmonic disturbance using proposed DSFT PLL control technique

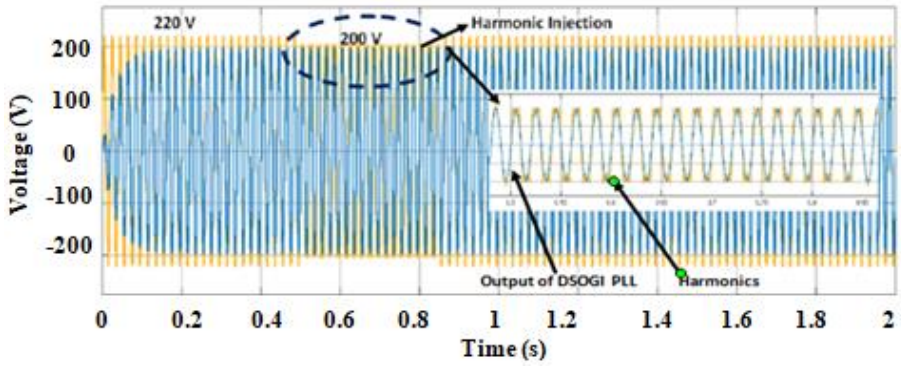

Fig. 14(b) Grid voltage with harmonic disturbance using DSOGI PLL control technique

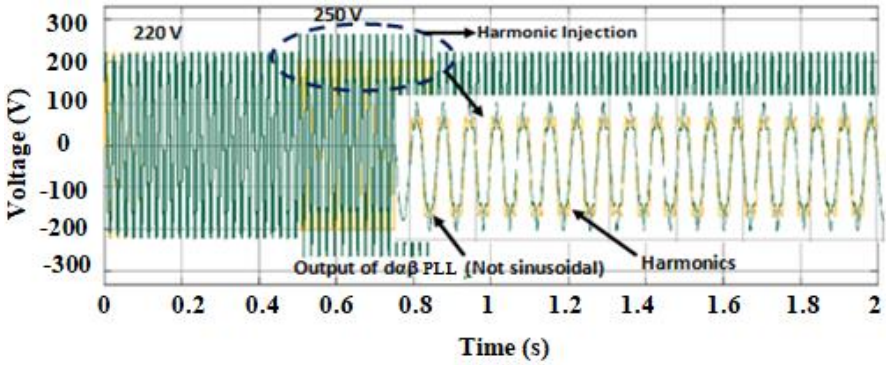

Fig. 14(c) Grid voltage with harmonic disturbance using dαβ PLL control technique

Fig. 14 Effect of PLL control techniques on the grid voltage with harmonic disturbance

The comparison results attained for the three control techniques i.e. DSFT PLL, DSOGI PLL and dαβ PLL on grid voltage with harmonic distortion has been tabulated in Table 3. It infers that the proposed DSFT strategy works better than DSOGI PLL and dαβ PLL techniques for the harmonic disturbance.

Table 3 Comparison of grid voltage for different control strategies in the presence of harmonic disturbance

Type of Disturbance	Control Strategy	Grid voltage during harmonic disturbance
Harmonic component injection	Proposed DSFT PLL	220 V
	DSOGI PLL	200 V
	dαβ PLL	250 V

4.3. Phase Jump Disturbance

In this paper, a shift of +90 degrees at 1.1 seconds and -90 degrees at 1.5 seconds has been considered. During this disturbance, the grid voltage undergoes a phase shift.

The grid voltage for phase A during the phase jump disturbance period is shown in Fig. 15.

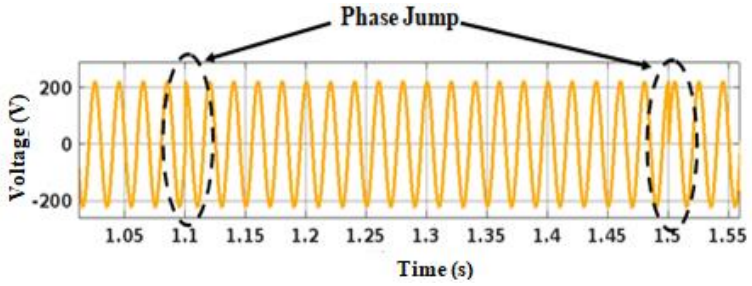

Fig. 15 Injection of Phase jump disturbance in grid voltage

Fig. 16 and Fig. 17 present the comparison of frequency and phase error for different PLL strategies considering phase jump disturbance, respectively. In Fig. 16, the DSFT PLL settles to 50 Hz frequency in 0.02 seconds, DSOGI PLL shows damped oscillations and, it hardly settles to the 50 Hz frequency, while dαβ PLL settles in 0.1 seconds to 50 Hz.

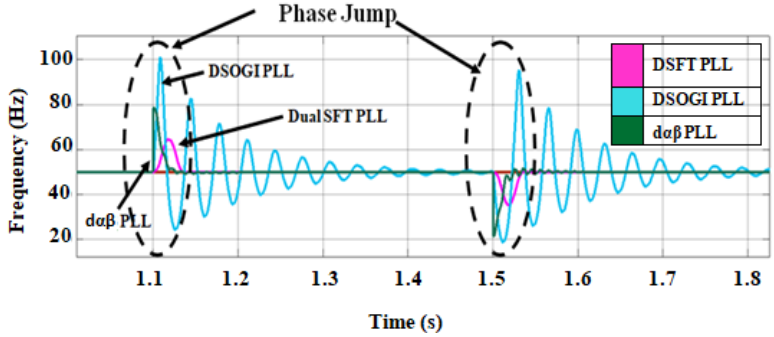

Fig. 16 Frequency comparison of PLL techniques with phase jump disturbance

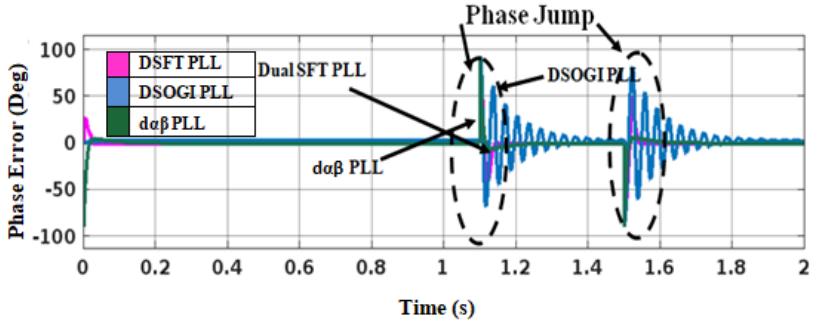

Fig. 17 Phase error comparison of PLL techniques with phase jump disturbance

The results obtained for proposed DSFT PLL, DSOGI PLL and dαβ PLL in terms of frequency tracking time and phase error settling time with phase jump disturbance is tabulated in Table 4.

Table 4 Comparison table for phase jump disturbance for frequency tracking and phase error settling time

Control Strategy	Frequency tracking time (Sec)	Phase Error Settling time (Sec)
Proposed DSFT PLL	0.02	0.02
DSOGI PLL	Damped oscillations	Damped oscillations
dαβ PLL	0.1	0.1

Table 4 clearly demonstrates that DSOGI PLL has damped oscillations, dαβ settles to zero error in 0.1 seconds while the proposed control technique DSFT PLL settles to zero phase error in only 0.02 seconds.

4.4. DC Offset Disturbance

In this type of disturbance, the DC offset value as presented in Fig. 18 gets added to the grid voltage. Here, the disturbance period ranges from 1.4 seconds to 1.65 seconds, during which 0.1*E (E is the peak of grid voltage) is added to phase A of grid voltage.

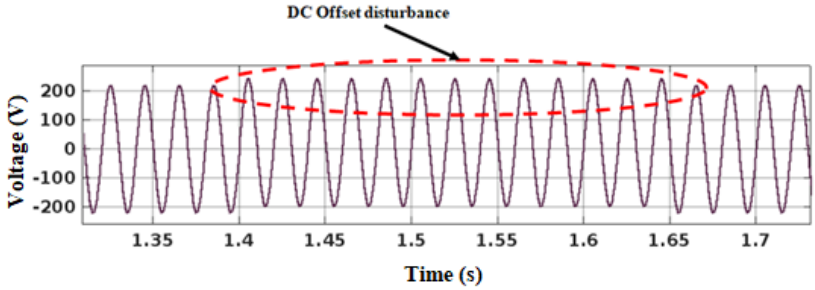

Fig. 18 Injection of DC offset disturbance in phase A of grid voltage

Fig. 19 illustrates the variation of frequencies in comparison with the original frequency kept at 50 Hz depicting that DSOGI PLL and dαβ PLL both results in oscillations. The oscillations of DSOGI PLL are much higher than dαβ PLL, whereas proposed DSFT PLL tracks 50 Hz frequency in 0.04 seconds.

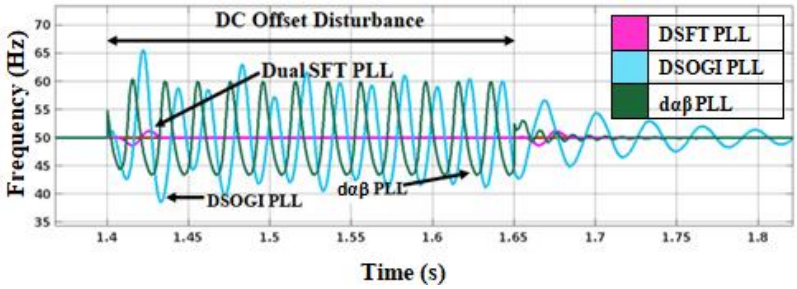

Fig. 19 Frequency comparison of PLL techniques with DC offset disturbance

The comparison of PLL techniques in terms of phase error settling time for DC offset disturbance is given in Fig. 20.

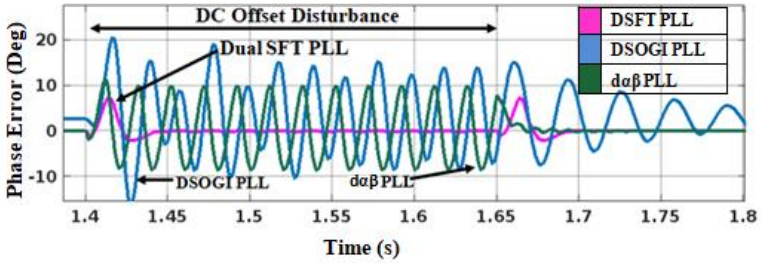

Fig. 20 Phase Error comparison of PLL techniques with DC offset disturbance

Table 5 presents the frequency tracking time and the phase error settling time of all the considered PLL techniques under the DC offset disturbance condition. It infers that DSOGI PLL and dαβ PLL both have oscillations. It also presents that DSFT PLL settles to zero phase error in 0.03 seconds and tracks 50Hz frequency in 0.04 seconds.

Table 5 Comparison of control strategies on frequency tracking time and phase error settling time with DC offset disturbance

Control Strategy	Frequency tracking time (Sec)	Phase error settling time (Sec)
Proposed DSFT PLL	0.04	0.03
DSOGI PLL	Oscillation	Oscillation
dαβ PLL	Oscillation	Oscillation

5. CONCLUSION

This paper meticulously examines the performance of a grid-connected PV system in the presence of a disturbed grid connection, specifically addressing four types of disturbances: frequency disturbance, harmonic disturbance, phase jump disturbance, and DC offset disturbance. The evaluation is based on key performance parameters, namely frequency tracking time and phase error settling time.

A novel proposed control strategy, Dual Sliding Fourier Transform (DSFT) Phase-Locked Loop (PLL), has been scrutinized under the influence of these disturbances and further compared against the conventional control strategies facing major drawbacks of large settling time, requirement of PID tuning, ineffectiveness in eliminating distortions, high frequency overshoots, namely, DSOGI PLL and dαβ PLL.

The uniqueness of the proposed system is underscored by its superior performance, demonstrating that the DSFT PLL control strategy surpasses the efficacy of the other control strategies. The proposed DSFT PLL avoids sustained oscillations and has shorter settling time over DSOGI PLL and dαβ PLL. The DSFT PLL effectively mitigates harmonics induced by grid disturbances, contributing to a cleaner signal and provides high immunity of the grid connected structure. Also, the strategy eliminates the necessity of PID controllers involving complex computations for tuning purposes**.**

These findings underscore the considerable potential of the proposed control strategy for enhancing the performance of grid-connected PV systems with grid disturbances implying a more reliable and resilient operation of solar power systems. The proposed strategy is versatile and can be extended to address multiple disturbances for real time applications such as faulty oscillations, low voltage ride-through and load fluctuations. This implies a broad applicability of the strategy. The economic feasibility of the proposed strategy can also be worked upon in future. The demonstrated novelty of the technique positions it as a valuable contribution to the field of grid-connected PV systems.

DECLARATIONS

On behalf of all authors, the corresponding author states that there is no conflict of interest. No funds, grants, or other support was received.

REFERENCES

[1] C.V. Nayar, S.M. Islam, H. Dehbonei, K. Tan, H. Sharma, "Power Electronics for Renewable Energy Sources", *Power Electronics Handbook*, 3rd ed., 2011, chapter 28, pp. 723–766.

[2] B. Stojčetović, M. Petković, M. and S. Đurović, "Assessment of renewable energy sources using mcdm method: case study", *Facta Universitatis, Series: Electronics and Energetics*, vol. 36, no. 3, pp. 353–363, 2023.

[3] N. Das, H. Wongsodihardjo, and S. Islam, "Modeling of multi-junction photovoltaic cell using MATLAB/Simulink to improve the conversion efficiency", *Ren. Energy*, vol. 74, pp. 917–924, 2015.

[4] P. Upadhyay, S. Pulipaka, M. Sharma, R. Kumar, "A proposed maximum power point operating strategy for photovoltaic applications using monthly irradiance estimates", *Sol. Energy*, vol. 141, pp. 266–277, 2017.

[5] M. Preradović, "Solar energy potential in Freiburg, Graz, Maribor, Banja Luka, Niš, and Athens", *Facta Universitatis, Series: Electronics and Energetics*, vol. 35, no. 3, pp. 393–403, 2022.

[6] A. Gupta, YK. Chauhan, RK.Pachauri, "A comparative investigation of maximum power point tracking methods for solar PV system", *Sol. Energy*, vol. 136, pp. 236–253, 2016.

[7] M. Jantsch, M. Real, H. Häberlin, C. Whitaker, K. Kurokawa, G. Blässer, P. Kremer and C.W.G. Verhoeve, "Measurement of PV maximum power point tracking performance", *Petten: Netherlands Energy Research Foundation* ECN,1997.

[8] D. L. King, "Photovoltaic module and array performance characterization methods for all system operating conditions", In Proceedings of the AIP conference, American Institute of Physics, 1997, vol. 394, no. 1, pp. 347–368, 1997.

[9] AJ. Carr, TL. Pryor, "A comparison of the performance of different PV module types in temperate climates", *Sol. energy*, vol. 76, no. 1–3, pp. 285–294, 2004.

[10] J.A. Eikelboom, and M.J. Jansen, Characterisation of PV modules new generations. *Results of tests and simulations*, 2000.

[11] P.M. Rooij, J.A. Eikelboom, and P.J.M. Heskes, "Reliability testing of grid connected PV inverters", *Netherlands Energy Research Foundation*, ECN, 2000.

[12] PVSSA. Parimala, D. Sharma, R. Mathew, "A comprehensive review on the advances in renewable wind power technology", *Wind Engineering*., vol. 47, no. 2, pp. 442–463, 2023.

[13] V.N. Kumar, N. Babu, R. Kiranmayi, P. Siano, and G. Panda, "Improved power quality in a solar PV plant integrated utility grid by employing a novel adaptive current regulator", *IEEE Systems Journal*, vol. 14, no. 3, pp. 4308–4319, 2019.

[14] S. K. Gupta, A. Aarti, and G. Diksha, "Comparison between inverter control techniques in grid connected solar photovoltaic systems", *Journal on Electrical Engg.*, vol. 12, no. 2, 2018.

[15] A. Aghazadeh, M. Davari, H. Nafisi, and F. Blaabjerg, "Grid integration of a dual two-level voltage-source inverter considering grid impedance and phase-locked loop", *IEEE J. Emerg. Sel. Topics Power Electron*., vol.9, no.1, pp. 401–422, 2021.

[16] P. Rodriguez, J. Pou, J. Bergas, J. I. Candela, R. P. Burgos, and D. Boroyevich, "Decoupled double synchronous reference frame PLL for power converters control", *IEEE Trans. Power Electron.*, vol. 22, no. 2, pp. 584–592, 2007.

[17] S. Golestan, S. Y. Mousazadeh, J. M. Guerrero, and J. C. Vasquez, "A critical examination of frequency-fixed second-order generalized integrator-based phase-locked loops", *IEEE Trans. Power Electron*., vol. 32, no. 9, pp. 6666–6672, 2017.

[18] J. Pinto, A. Carvalho, A. Rocha, A. Araújo, "Comparison of DSOGI-Based PLL for Phase Estimation in Three-Phase Weak Grids", *Electricity*, vol. 2, no.3, pp. 244–270, 2021.

[19] C. Zhang, X. Zhao, X. Wang, X. Chai, Z. Zhang, and X. Guo, "A grid synchronization PLL method based on mixed second- and thirdorder generalized integrator for DC offset elimination and frequency adaptability", *IEEE Trans. Emerg. Sel. Topics Power Electron.*, vol. 6, no. 3, pp. 1517–1526, 2018.

[20] M.P. Petronijević, Č. Milosavljević, B. Veselić, S. Huseinbegović, and B. Peruničić, "Discrete time quasi-sliding mode-based control of LCL grid inverters", *Facta Universitatis, Series: Electronics and Energetics*, vol. 36, no. 1, pp. 133–158, 2023.

[21] Z. Elkady, N. Abdel-Rahim, A. Mansour and F. Bendary, "Voltage Sag/Swell Detection Based on Decoupled Stationary Reference Frame PLL in DVR", In Proceedings of the 22nd International Middle East Power Systems Conference (MEPCON), Assiut, Egypt, 2021, pp. 678–682.

[22] N. Mohammed, W. Zhou, and B. Bahrani, "Comparison of PLL-Based and PLL-Less Control Strategies for Grid-Following Inverters Considering Time and Frequency Domain Analysis", *IEEE Access*, vol. 10, pp. 80518–80538, 2022.

[23] S.K. Chung, "A phase tracking system for three phase utility interface inverters", *IEEE Transactions on Power electronics*, vol. 15, no. 3, pp. 431–438, 2000.

[24] F. Sevilmiş, and H. Karaca, "Performance enhancement of DSOGI-PLL with a simple approach in grid-connected applications", *Energy Reports*, vol.8, pp. 9–18, 2022.
[25] K. Chandramohan, and K. Rajambal, "Performance evaluation of an intelligent decoupled stationary reference PLL for grid synchronization of five-phase wind power conversion system", *Jl. of Ambient Intelligence and Humanized Comp.*, pp. 1–17, 2020.
[26] S.K. Dash, and P.K. Ray, "Power quality improvement utilizing PV fed unified power quality conditioner based on UV-PI and PR-R controller", *CPSS Transactions on Power Electronics and Applications*, vol. 3, no. 3, pp. 243–253, 2018.
[27] B. Sahan, S. V. Araújo, C. Nöding and P. Zacharias, "Comparative Evaluation of Three-Phase Current Source Inverters for Grid Interfacing of Distributed and Renewable Energy Systems", *IEEE Transactions on Pow. Elec.*, vol. 26, no. 8, pp. 2304–2318, 2011.
[28] P. E. Schmid Jr, D. J. Nowak, and H. F. Harmuth, "Detection of orthogonal sine and cosine pulses by linear active RC-networks" *International Foundation for Telemetering*, 1967.
[29] S. A. Martucci, "Symmetric convolution and the discrete sine and cosine transforms", *IEEE Transactions on Signal Processing*, vol. 42, no. 5, pp. 1038–1051, May 1994.
[30] A. Bamigbade, V. Khadkikar, H. H. Zeineldin, M. S. E. Moursi and M. A. Hosani, "A Novel Power-Based Orthogonal Signal Generator for Single-Phase Systems", *IEEE Transactions on Power Delivery*, vol. 36, no. 1, pp. 469–472, Feb. 2021.
[31] V. N. Kumar, N. P. Babu, R. Kiranmayi, P. Siano, and G. Panda, "Improved power quality in a solar PV plant integrated utility grid by employing a novel adaptive current regulator", *IEEE Syst. J.*, vol. 14, no. 3, pp. 4308–4319, 2020.
[32] C. Yanarates and Z. Zhou, "Symmetrical Pole Placement Method-Based Unity Proportional Gain Resonant and Gain Scheduled Proportional (PR-P) Controller With Harmonic Compensator for Single Phase Grid-Connected PV Inverters", *IEEE Access*, vol. 9, pp. 93165–93181, 2021.
[33] K. Vidhya, & K. Krishnamoorthi, "A hybrid technique for optimal power quality enhancement in grid-connected photovoltaic interleaved inverter", *Energy & Environment*, 2022.